

## Performance Characteristics of Static and Dynamic Azimuthing Podded Propulsor

Mohammed F. Islam<sup>1</sup>, Ayhan Akinturk<sup>2</sup>, Brian Veitch<sup>3</sup> and Pengfei Liu<sup>2</sup>

<sup>1</sup>Oceanic Consulting Corporation (OCC), St. John's, NL, Canada

<sup>2</sup>Institute for Ocean Technology (IOT), National Research Council (NRC), St. John's, NL, Canada

<sup>3</sup>Faculty of Engineering, Memorial University of Newfoundland (MUN), St. John's, NL, Canada

### ABSTRACT

This paper presents results and analyses of an experimental study into the effects of static and dynamic azimuthing conditions on the propulsive characteristics of a puller podded unit in open water. The model propulsor was instrumented to measure thrust and torque of the propeller, three orthogonal forces and moments on the unit, rotational speed of the propeller, azimuthing angle and azimuthing rate. The model was first tested over a range of advance coefficients at various static azimuthing angles in the range of 0° to 360°. These tests were followed by tests in which the azimuthing angle was varied dynamically at different azimuthing rates and propeller rotational speeds. The performance coefficients of the propeller and the pod unit showed a strong dependence on the propeller loading and azimuthing angle. The open water characteristics were mostly irregular for the astern thrust conditions in the azimuthing angle beyond the range 90° to 270°, where the flow separation at the propeller blades and the pod-strut body might have occurred. The coefficients in static azimuthing conditions fit well with a 10<sup>th</sup> order polynomial fit of the data obtained in the dynamic azimuthing condition in the corresponding azimuthing angles and advance coefficients. An uncertainty analysis of the measurements is also presented.

### Keywords

Podded propulsor; static and dynamic azimuthing; propulsive performance; global forces and moments.

### 1 INTRODUCTION

Podded propulsors have the potential to become a popular main propulsion system because they allow more flexibility in design of the internal arrangement of a ship, potentially reduced noise and vibration, and increased manoeuvrability (Pakaste *et al.* 1999). Failures on early units led to a study about the sources of failure (Carlton 2002). This showed that bearings and seals were the sources of over one-half of the failures, thus highlighting the importance of predicting bearing and other propulsion forces accurately. A thorough investigation of the hydrodynamics behind the fluctuation of the bearing

forces and moments while operating in straight course and azimuthing conditions is required for a proper understanding of the issue.

There are a few recently published works that address the behaviour of podded propulsors at static and dynamic azimuthing angles: Szantyr (2001a and 2001b), Grygorowicz and Szantyr (2004), Woodward *et al.* (2004), Heinke (2004), Stettler (2004), Woodward (2006), Reichel (2007) and Wang (2007) are the most relevant ones. Szantyr (2001a and 2001b) published one of the first sets of systematic experimental data on podded propulsors as the main propulsion unit at static azimuthing angles. The study was limited to angles of  $\pm 15^\circ$ . Grygorowicz and Szantyr (2004) presented open-water measurements of podded propulsors both in puller and pusher configurations from tests in a circulating water channel. Heinke (2004) reported on comprehensive and systematic model test results, with a 4- and 5-bladed propeller fitted to a generic pod housing in pull- and push-modes. Stettler (2004), in his doctoral work investigated steady and unsteady dynamic manoeuvring forces associated with an azimuthing podded propulsor, and also provided supporting theoretical insight toward understanding their mechanisms and prediction. The work included quasi-steady vectored manoeuvring forces, of importance to all manoeuvring vehicles or ships, as well as unsteady or transient manoeuvring forces, which have more significance to the manoeuvrability of smaller vehicles, particularly for precision control applications. Woodward (2006) identified a few new methods for modelling the hydrodynamic reaction for both the ship hull and pod drive. A dedicated numerical simulation study was conducted exploring systematic variation of applied helm angles and comparison of time- and frequency-domain response. Reichel (2007) presented the preliminary part of comprehensive manoeuvring open water tests of a gas carrier model primarily focusing on open water experiments with an azimuthing podded propulsor. Wang (2007) performed a study to understand propeller-ice interaction phenomena and developed a numerical method to predict the interaction ice loads at different azimuthing conditions.

The present work reports on an experimental study of the forces and moments in the three coordinate directions and the propeller shaft thrust and torque of a model pod unit at different static and dynamic azimuthing conditions and propeller advance speeds in puller configuration. The work was the most recent part of a research program on podded propulsor performance. Amongst the hydrodynamic issues affecting performance that have been identified are questions regarding the effects of hub taper angle (Islam 2004, Islam *et al.* 2004, Islam *et al.* 2005, Islam *et al.* 2006a, Islam *et al.* 2006b, Islam 2006a, Taylor *et al.* 2005, Taylor 2006), pod-strut configuration (Islam 2004, Islam *et al.* 2006b, Taylor *et al.* 2005, Taylor 2006), pod-strut interactions (He *et al.* 2005a, He *et al.* 2005b, He 2006), pod-strut geometry (Molloy *et al.* 2005, Islam *et al.* 2006c), pod gap (Islam *et al.* 2007a), static azimuthing conditions (Islam *et al.* 2008b) and dynamic azimuthing conditions (Islam *et al.* 2007b).

## 2 METHOD, MODELS AND INSTRUMENT

In the current study, open water tests in straight course and azimuthing conditions were performed in accordance with the ITTC recommended procedure, Podded Propulsor Tests and Extrapolation (2002), and the description provided by Mewis (2001). The tests were performed using a custom-designed dynamometer and pod system.

In the tests, the propeller and unit performance were measured and analyzed at dynamically varying azimuthing angles under different operating conditions. Firstly, a dynamically-azimuthing podded propulsor was tested in puller configurations in open water conditions with  $0^\circ$  to  $360^\circ$  azimuthing. Secondly, the podded propulsor was tested at different static azimuthing angles for comparison purposes with the dynamic test results. The pod dynamometer system measured propeller shaft thrust ( $T_{Prop}$ ), propeller shaft torque ( $Q$ ), unit axial force ( $F_X$ ) and moment ( $M_X$ ), unit side/transverse force ( $F_Y$ ) and moment ( $M_Y$ ), and unit vertical force ( $F_Z$ ) and moment ( $M_Z$ ).

The pod unit with the propeller was rotated about the vertical axis passing through the centre of the strut in a continuous motion as the whole test unit moved forward with a specific advance and propeller shaft speeds. For the dynamic azimuthing study, the tests were done for dynamic azimuthing angles ranging from  $0^\circ$  to  $360^\circ$  at different azimuthing (steering) rates ( $2^\circ$ ,  $5^\circ$ ,  $10^\circ$ ,  $15^\circ$  and  $20^\circ$  per second) in puller configurations,  $0^\circ$  being the straight-ahead condition. Measurements were taken at different advance coefficients ranging from  $J=0.0$  to  $J=1.20$  at propeller rotational speed of 15 rps. The same pod unit was used to do the tests at different static azimuthing angles for comparison purposes with the dynamic test results. Table 1 shows the test matrix for the experiments. Most of the results presented in this paper involve the cases of advance coefficient of  $J=0.5$  (moderate loading condition).

**Table 1 Test matrix for systematic dynamic azimuthing podded propulsors' tests.**

Mode	Azimuth angle (degrees)	rps, n	Carriage speed (m/s)
Static azimuth	$0, \pm 5, \pm 10, \pm 15, \pm 20, \pm 30, \pm 45, \pm 60, \pm 90, \pm 120, \pm 150, \pm 160, \pm 170, \pm 175, 180$	15	0.0, 0.3, 0.45, 0.6, 0.75, 1.05, 1.2, 1.8, 2.1, 2.4, 2.7, 3.0, 3.3, 3.6
Dynamic azimuth	0 to 360 at different turning rates (2, 5, 10, 15, and 20 per seconds)	0, 8 and 15	0.0, 0.3, 0.45, 0.6, 0.75, 1.05, 1.2, 1.8, 2.1, 2.4, 2.7, 3.0, 3.3, 3.6

### 2.1 Pod and propeller models

The experiments included tests on a model propeller with a pod unit consisting of a pod shell and a strut. The propeller had a hub taper angle of  $-15^\circ$  (namely, Pull- $15^\circ$ ). The Pull- $15^\circ$  propeller was left-handed. A description of the propeller characteristics is provided in Table 2. Liu (2006) presented details of the geometry of the propellers.

**Table 2 Geometric characteristics of the propellers used in the current study.**

Diameter, $D_{Prop}$ (mm)	200
No. of blade	4
Design advance coefficient, $J$	0.8
Hub-Diameter ( $H/D$ ) ratio	0.26 (based on regular straight hub)
Shaft speed (rps)	15
Section thickness form	NACA 66 (DTMB Modified)
Section meanline	NACA = 0.8
Blade planform shape	Blade planform shape was based on David Taylor Model Basin model P4119
Expanded area ratio, $EAR$	0.60
Pitch distribution	Constant, $P/D=1.0$
Skew distribution	Zero
Rake distribution	Zero

The geometrical particulars of the pod unit (pod-strut and the propeller) used in the tests were defined using the parameters depicted in Figure 1. The values for the model propulsor were selected to provide an average representation of in-service, full-scale single-screw podded propulsors. The particulars of the pod-strut body are shown in Table 3.

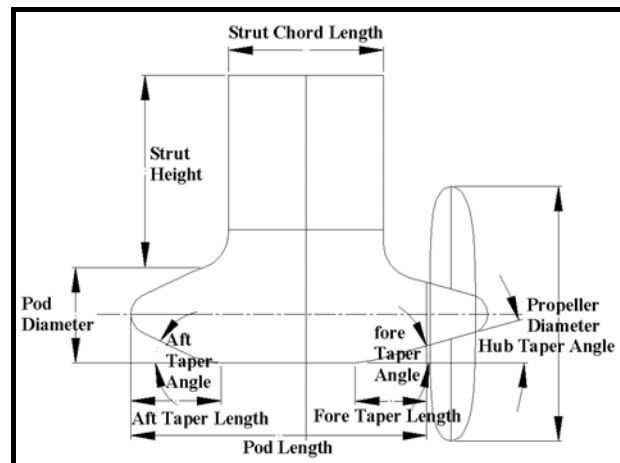


**Figure 1: Geometric parameters used to define pod-strut geometry.**

**Table 3: Pod-strut dimensions used in the current study.**

External Dimensions of Model Pod (mm)	
Propeller Diameter	200.0
Hub Angle (degrees)	15°
Pod Diameter	102.9
Pod Length	318.5
Strut Distance	74.1
Taper Length	81.5
Strut Length at Top	132.9
Strut Length at Pod	232.0

## 2.2 Experimental Apparatus and Approach

The current experiment was performed using a custom-designed dynamometer and pod system. The equipment has two major parts as shown in Figure 2. The pod dynamometer measures the thrust and the torque of the propeller at the propeller shaft very close to the hub. The global dynamometer measures the unit forces and moments in three coordinate directions. A motor mounted at the top of the global dynamometer drives the propeller shaft through an internal gear arrangement. Another motor arrangement mounted at the top of the seal plate (on the propeller boat, see below) turns the whole pod arrangement in a continuous motion over the horizontal plane (thus providing dynamic azimuthing). The six-component global dynamometer has three load cells measuring forces in the Z (vertically downward) direction; one load cell measuring forces in the X direction (in the direction of propeller advance) and two load cells measuring forces in the Y direction (across the propeller advance direction).

Figure 3 shows the propeller boat that was used to hold the pod dynamometer system. The boat protected the global unit and the data acquisition system from the water spray created by the pod unit. The boat was designed to be round so that it could be installed in any orientation and facilitate the installation of the pod units at any direction in the 360° horizon. This arrangement is specifically useful when two pods are tested simultaneously at any set-up of the pods (any lateral distance and alignment).

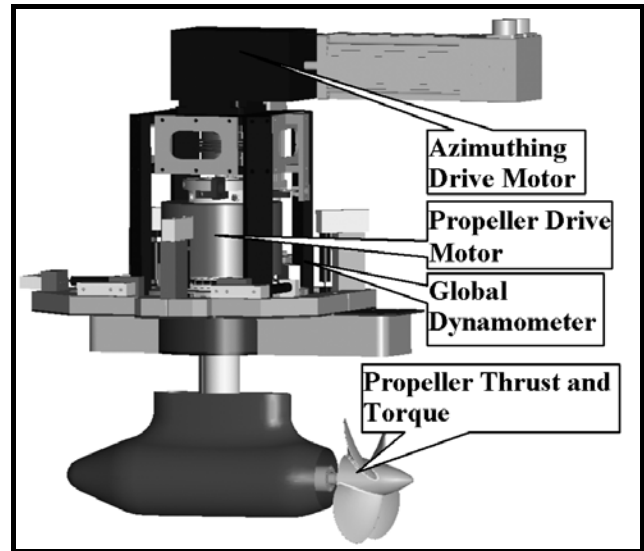


**Figure 2: Pod and the global dynamometer system designed and fabricated at IOT-NRC Canada.**

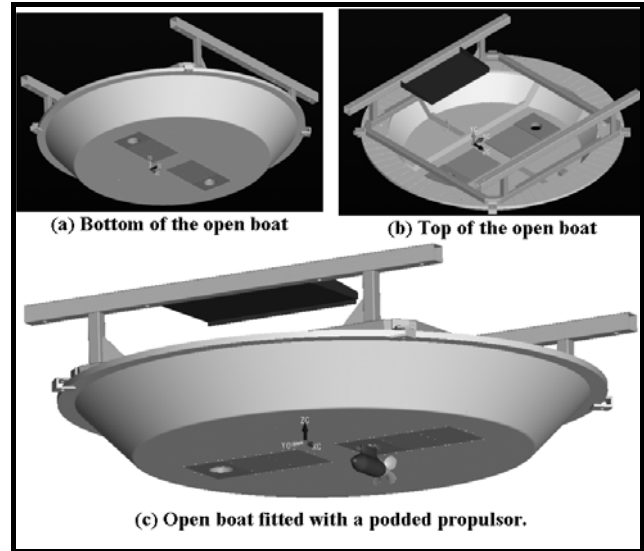


**Figure 3: The open boat to tests the podded propulsors, designed and fabricated at IOT-NRC Canada.**

The tests were performed in the 200m long towing tank facility resided in the National Research Council's Institute for Ocean Technology. The carriage is designed with a central testing area where a test frame, mounted to the carriage frame, allows the experimental setup to move transversely across the entire width of the tank. Figure 4 shows the pod dynamometer system installed in the IOT-NRC towing tank facility.



Figure 4: The pod dynamometer system installed in the IOT-NRC towing tank facility.

### 3 RESULTS AND DISCUSSIONS

The global dynamometer was calibrated by using the method described by Hess *et al.* (2000) and Galway (1980). The method takes into account cross-talk between the six load cells and produces an interaction matrix to convert the voltage output into the forces and moments in the three coordinate directions. The definition of the forces, moments and co-ordinates that was used to analyze the data and present the results is shown in Figure 5. The coordinate centre was situated 0.5m vertically above the pod centre, which is at the intersection of the horizontal axis through the propeller shaft centre and the vertical axis through the strut shaft centre. The propeller thrust and torque were measured at the propeller end of the shaft. The unit axial and side forces, and steering moment, are important from a steering and manoeuvring point of view, whereas the unit vertical force, axial and side moments, are important from a structural point of view. The unit vertical force and axial and side moments are not presented in this paper. The propeller forces, unit forces and moments are presented in the form of traditional non-dimensional coefficients as defined in Table 4.

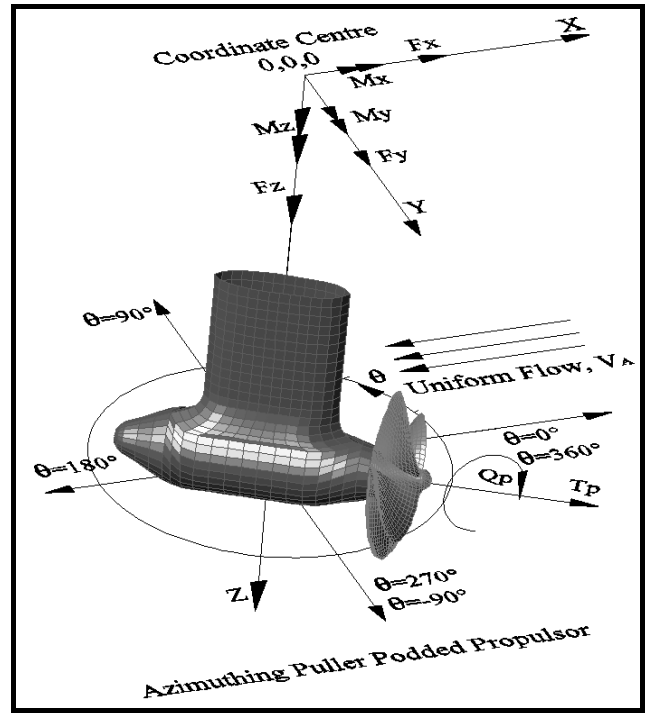


Figure 5: Definitions of forces, moments, coordinates of the puller azimuthing podded propulsor. Note that the unit forces and moments  $F_x, M_z$  etc. were measured at the global dynamometer which was 0.5 m above the centre of the pod.

Table 4: Data reduction equations and definitions of parameters used to present the experimental data.

Performance Characteristics	Data Equation	Reduction
$K_{T_{Prop}}$ – propeller thrust coefficient	$T_{Prop} / \rho n^2 D^4$	
$K_{T_{Unit}}$ – unit thrust coefficient,	$T_{Unit} / \rho n^2 D^4$	
$10K_Q$ – propeller torque coefficient	$10Q / \rho n^2 D^5$	
$J$ – propeller advance coefficient	$V_A / nD$	
$\eta_{Prop}$ – propeller efficiency	$J / 2\pi \times (K_{T_{Prop}} / K_Q)$	
$\eta_{Unit}$ – unit efficiency	$J / 2\pi \times (K_{T_{Unit}} / K_Q)$	
$K_{FZ}$ – transverse force coefficient	$F_Y / \rho n^2 D^4$	
$K_{FZ}$ – vertical force coefficient	$F_Z / \rho n^2 D^4$	
$K_{MX}$ – moment coefficient around x axis	$M_X / \rho n^2 D^5$	
$K_{MY}$ – moment coefficient around y axis	$M_Y / \rho n^2 D^5$	
$K_{MZ}$ – moment coefficient around z axis (steering moment)	$M_Z / \rho n^2 D^5$	

In the table,  $T_{Prop}$  is the propeller thrust;  $T_{Unit}$  is the unit thrust;  $Q$  is the propeller torque;  $\rho$  is the water density;  $n$  is the propeller rotational speed;  $D$  is the propeller diameter;  $V_A$  is the propeller advance speed, in the direction of carriage motion;  $F_{X,Y,Z}$  is the components of the hydrodynamic force on the pod unit in the three coordinate directions;  $M_{X,Y,Z}$  is the components of the hydrodynamic moment on the pod unit in the three coordinate directions. The propeller advance coefficient,  $J$ , is defined using the propeller advance speed,  $V_A$ , in the direction of carriage motion (in the direction of X in the inertia frame), not in the direction of the propeller axis.

However, the propeller thrust,  $T_{Prop}$ , and propeller torque,  $Q$ , are defined in the direction of the propeller axis.

### 3.1 Uncertainty of the Measurements

A brief discussion of the levels of uncertainty in the measurements is presented here. To assess the uncertainty in each set of experiments and to identify the major factors influencing these results, a thorough uncertainty analysis was conducted (Islam 2006a). The techniques used were based on adaptations of uncertainty analysis techniques outlined in ITTC recommended procedure (2002), Bose and Luznik (1996), Coleman and Steele (1999) and Hess *et al.* (2000). The uncertainty presented in the paper is only for the static azimuthing cases and no uncertainty analysis was carried out for the dynamic azimuthing cases.

The overall uncertainty in the non-dimensional performance coefficients of the podded propulsors required proper identification of all the variables contained within the data reduction expressions Coleman and Steele (1999). The experimental approaches used to obtain the data for each of the variables in the expressions were influenced by a variety of elemental sources of error. These elemental sources were estimated, and combined using the root-sum-square (RSS) method to give the bias and precision limits for each of the variables. The bias errors consisted of many elemental sources of error, which depended on the approaches followed to measure the variables. However, for the precision error estimates of most variables, only one source of error (repeatability) was considered significant. In order to calculate the uncertainty due to calibration of the six-component dynamometer measurement, it was required to determine how the uncertainties in the calibration data propagates into each element of the interaction matrix and into the measured forces and moments (Hess *et al.* 2000).

The error estimates used in the determination of the bias and precision errors in this study were considered to be 95% coverage estimates. The bias uncertainty and the precision uncertainty were combined using the root-sum-square (RSS) method to provide estimates of overall uncertainty levels in these variables. The overall uncertainty was thus considered to be a 95% coverage estimate.

The final step in the methodology of uncertainty analysis was to determine how uncertainties in each of the variables propagate through the data reduction equations. Using the approaches described in Bose and Luznik (1996), Coleman and Steele (1999) and Hess *et al.* (2000), the uncertainty expressions for each set of experiments were developed as shown in equation 1 to 6, where  $U$  denotes the uncertainties in the corresponding coefficients denoted by the subscripts. In deriving the expressions, the cross-correlated bias limits were ignored Bose and Luznik (1996). Strictly they should have been included, but they would have, in the current case, reduced the total uncertainty.

$$\left(\frac{U_{K_{TProp}}}{K_{TProp}}\right)^2 = \left(\frac{U_{TProp}}{T_{Prop}}\right)^2 + \left(\frac{U_{\rho}}{\rho}\right)^2 + 4\left(\frac{U_n}{n}\right)^2 + 16\left(\frac{U_D}{D}\right)^2 \quad (1)$$

$$\left(\frac{U_{K_Q}}{K_Q}\right)^2 = \left(\frac{U_Q}{Q}\right)^2 + \left(\frac{U_{\rho}}{\rho}\right)^2 + 4\left(\frac{U_n}{n}\right)^2 + 25\left(\frac{U_D}{D}\right)^2 \quad (2)$$

$$\left(\frac{U_{K_{TUnit}}}{K_{TUnit}}\right)^2 = \left(\frac{U_{TUnit}}{T_{Unit}}\right)^2 + \left(\frac{U_{\rho}}{\rho}\right)^2 + 4\left(\frac{U_n}{n}\right)^2 + 16\left(\frac{U_D}{D}\right)^2 \quad (3)$$

$$\left(\frac{U_{K_{Fy}}}{K_{Fy}}\right)^2 = \left(\frac{U_{Fy}}{F_y}\right)^2 + \left(\frac{U_{\rho}}{\rho}\right)^2 + 4\left(\frac{U_n}{n}\right)^2 + 16\left(\frac{U_D}{D}\right)^2 \quad (4)$$

$$\left(\frac{U_{K_{Mz}}}{K_{Mz}}\right)^2 = \left(\frac{U_{Mz}}{M_z}\right)^2 + \left(\frac{U_{\rho}}{\rho}\right)^2 + 4\left(\frac{U_n}{n}\right)^2 + 25\left(\frac{U_D}{D}\right)^2 \quad (5)$$

$$\left(\frac{U_J}{J}\right)^2 = \left(\frac{U_{V_A}}{V_A}\right)^2 + \left(\frac{U_n}{n}\right)^2 + \left(\frac{U_D}{D}\right)^2 \quad (6)$$

In the expressions for the podded propulsor tests, for both thrust and torque coefficient uncertainties, the tare thrust and frictional torque were embedded in the corresponding measurements. Since the tare thrust and frictional torque were part of the same data stream as the thrust and torque readings, they were not treated as an independent contributor of error to the corresponding coefficients, but rather as a bias error on the static-zero value of the thrust and the torque measurements. The resulting error estimates for the podded propulsor tests are given in Table 6 and 7 as a percentage of the performance coefficients at same loading condition. The uncertainty estimates were based on the test and calibration data presented in the reports by Islam (2006a, 2006b and 2006c).

**Table 6: Overall uncertainties in advance coefficient, propeller thrust and torque coefficients and unit thrust coefficient for the podded propulsor.**

Advance Coefficient Value	Advance Coefficient Error (+/-)	Propeller Thrust Coefficient Error (+/-)	Propeller Torque Coefficient Error (+/-)	Unit Thrust Coefficient Error (+/-)
0.00	-	2.54	1.62	0.90
0.20	1.02	2.90	1.79	0.91
0.40	0.59	3.53	2.05	0.94
0.60	0.47	4.68	2.51	1.00
0.70	0.44	5.61	2.86	1.05
0.80	0.42	7.16	3.47	1.16
0.90	0.40	9.96	4.42	1.47
1.00	0.39	16.93	6.33	3.50
1.10	0.38	72.98	12.83	3.87
1.20	0.38	28.16	82.33	1.65

**Table 7: Overall uncertainties in global force and moment coefficients in the three orthogonal directions for the podded propulsor.**

Advance Coefficient Value	Trans. Force Coefficient	Vertical Force Coefficient Error	Axial Moment Coefficient Error	Vertical Moment Coefficient Error	Steering Moment Coefficient Error

	Error (+/-)	(+/-)	(+/-)	(+/-)	(+/-)
0.00	110.94	633.92	1.34	0.86	4.90
0.20	31.81	100.09	1.30	0.86	4.79
0.40	15.01	53.09	1.28	0.87	5.53
0.60	8.73	37.10	1.33	0.91	5.80
0.70	7.00	25.16	1.39	0.93	6.14
0.80	6.07	14.76	1.53	0.99	6.65
0.90	5.75	6.88	1.82	1.16	8.30
1.00	6.82	1.98	2.51	2.47	10.44
1.10	30.32	5.77	7.14	2.77	20.06
1.20	26.00	9.95	6.90	1.34	1655.98

The primary element of the uncertainty of the propeller performance coefficients was the bias error (80% or more of the total uncertainty for the pod dynamometer system). To reduce the overall uncertainty in the final results, the primary focus should be to reduce the bias error in the equipment. However, for the global performance coefficients, generally, the primary element of the uncertainty was precision error (about 70% or less of the total uncertainty).

Applying the uncertainty limits to the performance curves of pod unit in the form of error bars results in a plot as shown in Figure 6. It is observed in the figure that the curves fitted to the data lie inside the error bars. Therefore, the fitted curves provide a good representation of the trends indicated by the results. The custom-made podded propulsor dynamometer system demonstrated the capability of achieving uncertainty limits close to those of commercial standard equipment.

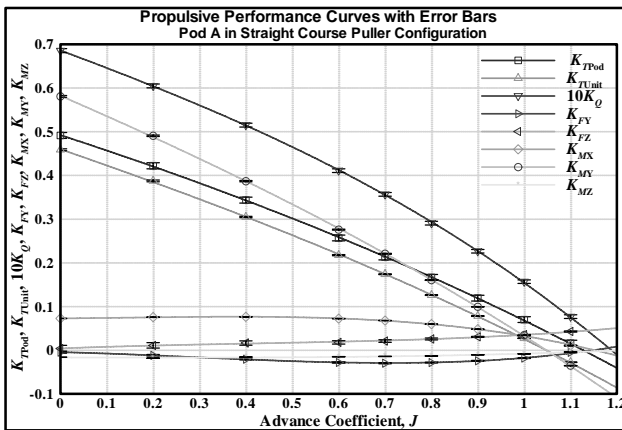


Figure 6 Performance curves for the pod (200 mm propeller diameter) in straight-course puller configuration with uncertainty (error) bars.

### 3.1 Effect of Dynamic Azimuthing

A comparative study was made between the measurements obtained in the static and dynamic azimuthing cases in the corresponding operating condition. An azimuthing rate of 10°/sec was used in this part of the study. A 10<sup>th</sup> order polynomial fit was used to represent the mean level of the dynamic test data to facilitate the comparison of the static and dynamic test results at corresponding operating conditions. The comparison at an advance coefficient value of 0.5

(moderate advance coefficient) is presented in this paper. In each of the figures in this section, black solid circle represents the average of the performance coefficients at static azimuthing conditions, black dots represents the raw unfiltered data and black solid line represents the 10<sup>th</sup> order polynomial fit to the raw data in the dynamic azimuthing conditions.

Figures 7 and 8 show a comparison of the propeller thrust and torque coefficients between the static and dynamic azimuthing conditions in the azimuthing range from 0° to 360° and at advance coefficient of  $J= 0.5$ , respectively. Both the thrust and torque coefficients at static azimuthing conditions fell close to the polynomial curve fit for the dynamic azimuthing data. Thus, the mean values of the static case coincide well with the mean values the dynamic azimuthing results. The minor differences were mostly observed in the astern thrust condition (between 120° to 240°) and can be attributed to the uncertainty in the measurements. The fit under estimates the second peak for of the static case at around 250°.

For both static and dynamic cases, the propeller thrust and torque coefficients of the puller propeller increased when the azimuthing angles were increased from straight-ahead condition (0° angle) both in positive and negative azimuthing angles. The maximum propeller coefficients were observed at the approximate azimuthing angles of 120° and 240°. There was some scatter at the large azimuthing angles, which can be attributed to the unsteady nature of the reverse wash and separation (at azimuthing angles between 120° and 240°). Propeller thrust and torque coefficient showed similar trends at corresponding azimuthing angles and advance coefficients. The fluctuations in the magnitude of both the thrust and the torque coefficients (the shaded area in the figures) for the advance coefficient show that in dynamic azimuthing conditions, the propeller thrust and torque fluctuate over a considerable range and care should be taken in designing the propeller bearings which would be subjected to this kind of fluctuation force. The fluctuations observed in the dynamic case can be attributed to two main sources: propeller rotation and dynamic azimuthing. A further explanation of the fluctuation in the dynamic case is provided in the next section.

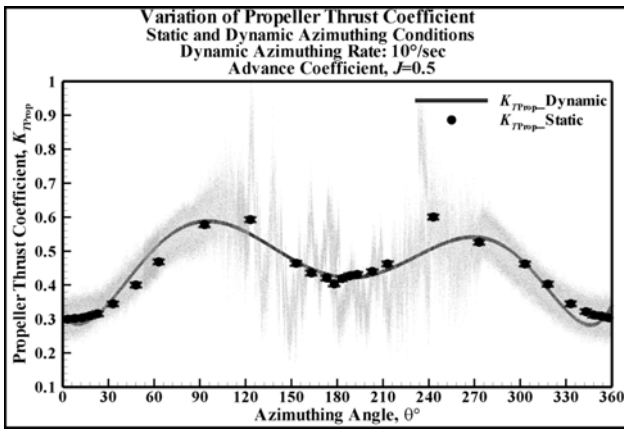


Figure 7 Experimental results: comparison of propeller thrust coefficient of the model pod unit at static and dynamic azimuthing conditions and at advance coefficient of 0.5.

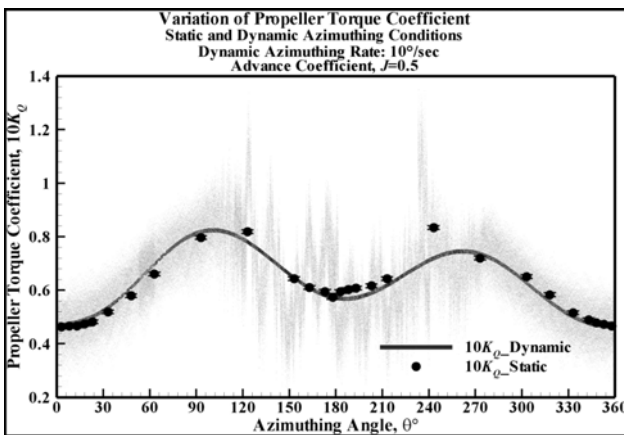


Figure 8 Experimental results: comparison of propeller torque coefficient of the model pod unit at static and dynamic azimuthing conditions and at advance coefficient of 0.5.

A similar comparison was made for unit thrust, transverse force and steering moment coefficient of the entire pod unit and are shown in Figures 9 to 11. The mean force coefficients at static azimuthing conditions compare well with the 10<sup>th</sup> order polynomial fit to the dynamic azimuthing data for most of the azimuthing angles. High fluctuations in the magnitude of these global force and moment coefficients were observed, specifically in the range of azimuthing angles between 90° to 270° (reverse wash condition). Similarly to the other force coefficients mentioned above, the discrepancy observed  $J = 0.5$  in the range of azimuthing angle from 90° to 270° can be attributed to the unsteady nature of the operating condition and to the polynomial fit used.

The unit thrust coefficients, Figure 9, decreased for both azimuthing directions but the reduction was visibly stronger for negative azimuthing angles. A similar trend was found for all advance coefficients and within the range of azimuthing angles between 90° and 270°. The unit thrust coefficients increased as the azimuthing angle was increased further beyond 90° and below 270°. The minor asymmetry that was seen in the corresponding

azimuthing angles in the port and starboard side (30° and 330°, for example) can be primarily attributed to the direction of rotation of the propeller and measurement error.

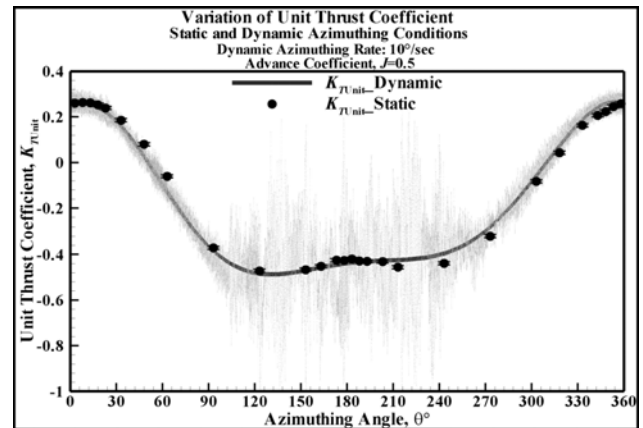


Figure 9 Experimental results: comparison of unit thrust coefficient of the model pod unit at static and dynamic azimuthing conditions and at advance coefficient of 0.5.

The transverse force coefficient, Figure 10, of the propulsor with left-handed propeller showed strong dependency on propeller loading and azimuthing angle. For the advance coefficient, the transverse force coefficients increased with both positive and negative azimuthing angles from straight-ahead condition. The maximum transverse force coefficient was found in the range of 60° to 90° and 270° to 300°, depending on the direction of rotation of the pod unit. For small azimuthing angle (less than 45°), the trend of the transverse force was similar to that of a classic rudder.

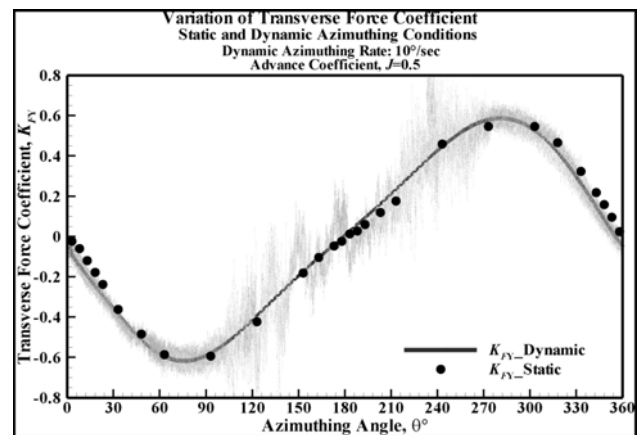


Figure 10 Experimental results: comparison of transverse force coefficient of the model pod unit at static and dynamic azimuthing conditions and at advance coefficient of 0.5.

The steering moment coefficient, Figure 11, showed nonlinear changes with advance coefficients and azimuthing angle. The steering moment coefficient increased with the larger azimuthing angles up to 90° or 270°. For further increase in azimuthing angle up to ±180°, a decrease in steering moment was observed. The fluctuation of the magnitude of the steering moment coefficient for both advance coefficients shows that at dynamic azimuthing conditions, the steering moment

fluctuates within a considerable range and this should be taken into account when designing the radial/slewing bearing, which would have to resist these large fluctuating moments.

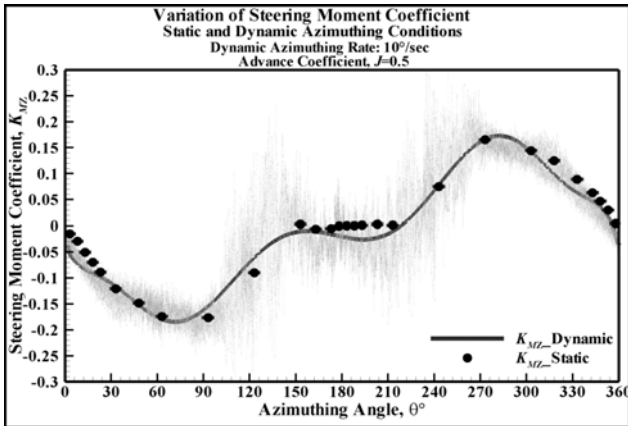


Figure 11 Experimental results: comparison of steering moment coefficient of the model pod unit at static and dynamic azimuthing conditions and at advance coefficient of 0.5.

### 3.2 Fluctuations of Forces and Moments

Figure 12 compares the fluctuations in the magnitude of the propeller thrust coefficient for static and dynamic azimuthing conditions at some high azimuthing angles and at an advance coefficient of  $J=0.5$ . It shows that both in static and dynamic azimuthing conditions, the propeller thrust fluctuated over a considerable range. In the figure, the oval markers indicate 5 azimuthing angles in dynamic condition and those are related to the unfiltered data for the corresponding static azimuthing angles. This illustrates the level of fluctuations observed in the two cases.

Overall, for all forces and moments and especially in the reverse wash conditions ( $90^\circ$  to  $270^\circ$ ), large fluctuations of forces and moments in the form of spikes were observed. The range of fluctuation of the forces and moments in the static azimuthing tests (for a fixed advance coefficient) was slightly lower than that in the dynamic azimuthing tests in the corresponding operating conditions especially in the reverse wash conditions. This difference can either be a reality or an uncertainty inherent to the measurements. A further study in evaluating the uncertainty of the measurements in the dynamic azimuthing cases is required to justify this difference.

This form of fluctuating loads was reported in the study by Woodward (2006). Woodward found that these spike loads do not influence the manoeuvring response assessment and have only a minor impact on the manoeuvring response itself. Nevertheless, the spike loads have a significant impact on the structure, shaft and stock bearings and other related systems. Thus, careful attention should be paid to the manoeuvring related design and operational implications, to better understand and control the influence of the spike loads experienced

by pod drives (Woodward 2006).

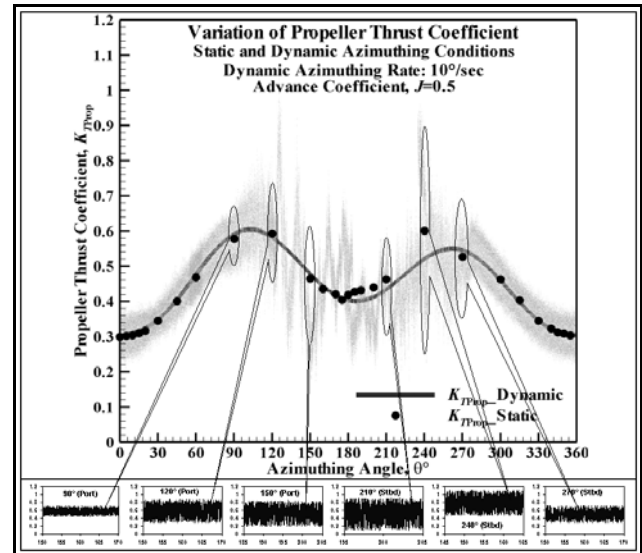
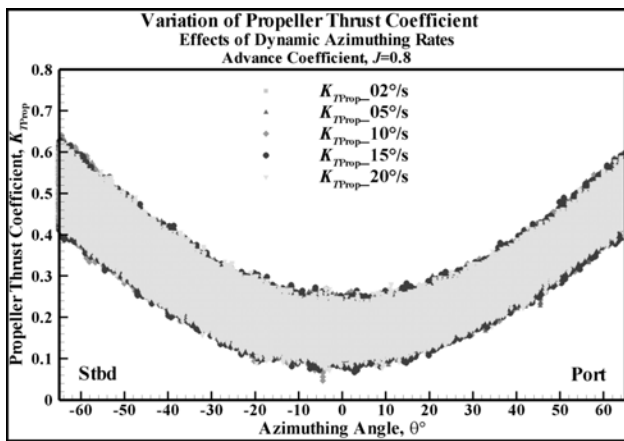


Figure 12 Experimental results: comparison of propeller thrust coefficient of the model pod unit at static (black solid circle) and dynamic azimuthing conditions (black dots for raw unfiltered data and black solid line for 10<sup>th</sup> order polynomial fit to the raw data).

### 3.3 Effects of Azimuthing Rate

The study into the effect of azimuthing rate on the propeller and unit forces and moments at dynamic azimuthing conditions within the range of  $+60^\circ$  to  $-60^\circ$  was carried out for the advance coefficient of  $J = 0.8$ . The performance coefficients were measured at azimuthing rates of  $2^\circ/\text{sec}$ ,  $5^\circ/\text{sec}$ ,  $10^\circ/\text{sec}$ ,  $15^\circ/\text{sec}$ , and  $20^\circ/\text{sec}$  for the above operating conditions. The original unfiltered data, Figure 13, at different azimuthing rates was too hard to distinguish from each other. It can be observed that the difference between the performance coefficients with the change of azimuthing rate was within the error limits found in the uncertainty analysis. Also, the uncertainty analysis was carried out only in static conditions, which may not be applicable in the dynamic cases. Based on the current analysis, it was concluded that azimuthing rate did not have noticeable effect on the performance coefficients with the change of azimuthing angle in dynamic operating condition. Further study in such kind should be accompanied by an uncertainty analysis in the dynamic cases.



**Figure 13: Experimental results: Original unfiltered data showing the variation of propeller thrust coefficient of the model pod unit with azimuthing rate in dynamic conditions.**

#### 4 CONCLUDING REMARKS

An experimental study of shaft thrust and torque, unit thrust and transverse force, and steering moment, of a model pod unit at different static and dynamic azimuthing conditions and advance coefficients was for puller configuration in open water. A custom-made dynamometer system was used to measure forces and moments of the pod unit at different dynamic azimuthing conditions in the range of  $0^\circ$  to  $360^\circ$  azimuthing positions. The results supply some fundamental information with respect to manoeuvring loads from the pod and also a base for the validation of numerical modeling.

The propeller thrust and torque coefficients of the puller propeller increased when the azimuthing angles were increased from straight-ahead condition ( $0^\circ$  angle) both in positive and negative azimuthing angles. The maximum propeller coefficients were observed at the azimuthing angles of  $120^\circ$  and  $240^\circ$ . Propeller thrust and torque coefficient showed similar trends at corresponding azimuthing angles and advance coefficients.

The unit thrust coefficients decreased for both azimuthing directions but the reduction was visibly stronger for negative azimuthing angles. A similar trend was found for all advance coefficients and within the range of azimuthing angles of  $90^\circ$  and  $270^\circ$ . The unit thrust coefficients increased as the azimuthing angle was increased further beyond  $90^\circ$  and decreased from  $270^\circ$ .

The transverse force coefficient of the propulsor with left-handed propeller showed strong dependency on propeller loading and azimuthing angle. For the advance coefficient, the transverse force coefficients increased with both positive and negative azimuthing angles from straight-ahead condition. The maximum transverse force coefficient was found in the range of  $60^\circ$  to  $90^\circ$ .

The steering moment coefficient showed nonlinear changes with advance coefficients and azimuthing angle.

The comparative study of the propeller thrust and torque coefficients and unit forces and moments between the static and dynamic azimuthing conditions in the

azimuthing range from  $0^\circ$  to  $360^\circ$  and at advance coefficient of 0.5 shows that the performance coefficients at static azimuthing conditions coincided well with the 10<sup>th</sup> order polynomial curve fit for the dynamic azimuthing data. The discrepancy observed in the range of azimuthing angles from  $120^\circ$  to  $270^\circ$  might be attributed to the unsteady nature of the operating condition. In dynamic azimuthing conditions, the fluctuation of the magnitude of the performance coefficients for both advance coefficients showed a considerable range and care should be taken while designing the propeller and pod bearings, which would be subjected to the fluctuating forces.

The azimuthing rate did not have any significant effect of the performance coefficients with the change of azimuthing angle at a fixed advance coefficient. The minor difference found might be attributed to the uncertainty in the measurements.

The uncertainty analysis results provided strong evidence that the experimental data obtained using the pod dynamometer system presented the true performance characteristics of the model scale podded propulsors under consideration.

#### ACKNOWLEDGEMENTS

This study on podded propellers is a Joint project between the National Research Council of Canada, Transport Canada and Memorial University. The authors thank Mr. Victor Santos-Pedro, Director, Design, Equipment and Boating Safety, Marine Safety, Transport Canada for continued support of in this research. Special thanks are extended to the members of Design and Fabrication and Experimental Facilities at the National Research Council of Canada's Institute for Ocean Technology.

#### REFERENCES

- Carlton, J. S. (2002). 'Podded Propulsors: some design and service experience'. The Motor Ship Marine Propulsion Conference. Copenhagen, Denmark, April 9-10, 7p.
- Coleman, H. W. and Steele, W. G. (1999). Experimentation and uncertainty analysis for engineers. Wiley Interscience.
- Galway, R. D. (1980). A comparison of methods for calibration and use of multi-component strain gauge wind tunnel balances. Aeronautical Report LR-600, NRC No. 18227, National Aeronautical Establishment, National Research Council, Canada, 40p.
- Grygorowicz, M. and Szantyr, J. A. (2004). 'Open water experiments with two pods propulsor models'. In Proceedings of the 1st International Conference on Technological Advances in Podded Propulsion. Newcastle University, UK, April, pp. 357-370.
- He, M., Veitch, B., Bose, N., Bruce, C., and Liu, P. (2005a). 'Numerical simulations of propeller wake

- impacting on a strut'. In proceedings of the CFD2005. St John's, NL Canada, August, 8p.
- He, M., Veitch, B., Bose, N. and Liu, P. (2005b). 'An investigation on wake/strut interaction of a tractor-Type podded propulsor'. In proceedings of the 7<sup>th</sup> CMHSC. Halifax, NS Canada, September 21-22, 8p.
- He, M. (2006) 'Propeller wake impingement on a strut'. PhD thesis. Faculty of Engineering and applied Science, Memorial University of Newfoundland, 250p.
- Heinke, H. J. (2004). 'Investigation about the forces and moments at podded drives'. In Proceedings of the 1st International Conference on Technological Advances in Podded Propulsion. Newcastle University, UK, April, pp. 305-320.
- Hess, D.E., Nigon, R.T. and Bedel, J. W. (2000). 'Dynamometer calibration and usage, Research and Development'. Report No. NSWCCD-50-TR-2000/040. Hydromechanics Directorate, Carderrock Division, Naval Surface Warfare Centre, West Bethesda, Maryland, 31p.
- Islam, M. F. (2004). 'Numerical investigation on effects of hub taper angle and pod-strut geometry on propulsive performance of pusher propeller configurations'. Master of Engineering thesis. Memorial University of Newfoundland, Canada, 136 p.
- Islam, M. F., Taylor, R., Quinton, J., Veitch, B., Bose, N., Colbourne, B., and Liu, P. (2004). 'Numerical investigation of propulsive characteristics of podded propeller'. In proceedings of the 1st International Conference on Technological Advances in Podded Propulsion. Newcastle University, UK, April, pp. 513-525.
- Islam, M. F., Veitch, B., Bose, N., and Liu, P. (2005). 'Cavitation characteristics of pushing and pulling podded propellers with different hub taper angles'. In proceedings of the 7<sup>th</sup> CMHSC. Halifax, NS Canada, September 21-22, 7p.
- Islam, M. F. (2006a). 'Uncertainty analysis of NSERC-NRC pod dynamometer system'. Ocean Engineering Research Centre (OERC) Report No. OERC-2006-05. St. John's, NL, Canada, 96p.
- Islam, M. F. (2006b). 'Calibration and usages of NSERC-NRC pod dynamometer system'. Ocean Engineering Research Centre (OERC) Report No. OERC-2006-04. St. John's, NL, Canada, 2006, 80p.
- Islam, M. F. (2006c). 'Cavitation performance testing of podded propellers with different hub taper angles'. Ocean Engineering Research Centre (OERC) Report No. OERC-2006-03, St. John's, NL, Canada, 2006, 62p.
- Islam, M. F., Veitch, B., Bose, N., and Liu, P. (2006a). 'Numerical study of hub taper angle on podded propeller performance'. Journal of Marine Technology. Vol. 43, No. 1, pp. 1-10.
- Islam, M. F., Veitch, B., Bose, N., and Liu, P. (2006b). 'Hydrodynamic characteristics of pod propeller units of highly tapered hub'. In proceedings, Propellers/Shafting, Society of Naval Architects and Marine Engineers. Virginia Beach, USA, 12p.
- Islam, M. F., Molloy, S., He, M., Veitch, B., Bose, N., and Liu, P. (2006c). 'Hydrodynamic study of podded propulsors with systematically varied geometry'. In proceedings of the 2<sup>nd</sup> International Conference on Technological Advances in Podded Propulsion. Brest, France, 14p.
- Islam, M. F., MacNeill A., Veitch B., Akinturk A., and Liu P. (2007a). 'Gap effect on performance of podded propulsors in straight and static azimuthing conditions'. In proceedings of the 8<sup>th</sup> CMHSC 2007. St. John's, Canada, 9p.
- Islam, M. F., Akinturk A., Veitch B., and Liu P. (2007b). 'Performance characteristics of a podded propulsor during dynamic azimuthing'. In proceedings of the 8<sup>th</sup> CMHSC 2007. St. John's, Canada, 8p.
- Islam, M. F., Veitch B, Molloy S, Bose N, and Liu P. (2008a). 'Effects of geometry variations on the performance of podded propulsors'. To be appeared in SNAME Transaction. Florida, USA, 17p.
- Islam, M. F., Veitch B., Akinturk A., Bose N., and Liu P. (2008b). 'Performance study of podded propulsor in static azimuthing conditions'. being reviewed in the Journal of International Shipbuilding Progress. 15p.
- ITTC – Recommended Procedures. (2002). 'Propulsion, Performance - Podded Propeller Tests and Extrapolation'. 7.5-02-03-01.3, Revision 00.
- Liu, P. (2006). 'The design of a podded propeller base model geometry and prediction of its hydrodynamics'. Technical Report no. TR-2006-16. Institute for Ocean Technology, National Research Council, Canada, 16p.
- Mewis, F. (2001). 'The efficiency of pod propulsion'. HADMAR 2001. Bulgaria, October, 7p.
- Molloy, S., Islam, M. F., He, M., Veitch, B., Bose, N., Wang, J., Akinturk, A., and Liu, P. (2005). 'Use of factorial design in podded propulsors geometric series'. In proceedings of the 7<sup>th</sup> CMHSC. Halifax, NS Canada, September 21-22, 8 p.
- Pakaste, R., Laukia, K., Wilhelmson, M. (1999). 'Experience with Azipod® Propulsion Systems on Board Marine Vessels'. ABB Review, Issue 2, 12p.
- Reichel, M. (2007). 'Manoeuvring forces on azimuthing podded propulsor model'. Polish Maritime Research. Versita, ISSN: 1233-2585, Vol. 14, No. 2, pp 3-8.
- Stettler, J. W. (2004). 'Steady and unsteady dynamics of an azimuthing podded propulsor related to vehicle maneuvering'. PhD thesis. Massachusetts Institute of Technology, 187p.

- Szantyr, J. A. (2001a). 'Hydrodynamic model experiments with pod propulsor'. International symposium of ship propulsion (Lavrentiev Lectures). State Marine Technical University, St. Petersburg, Russia, pp. 95-104.
- Szantyr, J. A. (2001b). 'Hydrodynamic model experiments with pod propulsor'. Oceanic Engineering International. Vol. 5, No.2, pp. 95-103.
- Taylor, R. (2006). 'Experimental investigation of the influence of hub taper angle on the performance of push and pull configuration podded propellers'. Master's of Engineering Thesis. Memorial University of Newfoundland, Canada, 120p.
- Taylor, R. Veitch, B., and Bose, N. (2005). 'The influence of hub taper angle on podded propeller performance: 'propeller only' tests vs. 'podded propeller unit' tests'. In proceedings of the 7<sup>th</sup> CMHSC. Halifax, NS Canada, September 21-22, 8p.
- Wang, J. (2007). 'Prediction of propeller performance on a model podded propulsor in ice (propeller-ice interaction)'. PhD thesis. Faculty of Engineering and Applied Science, Memorial University of Newfoundland, Canada, 251p.
- Woodward, M. D. (2006). 'Steady control and response of pod driven ships'. PhD thesis. School of Marine Science and Technology, University of Newcastle-upon-Tyne, 255p.
- Woodward, M.D., Atlar, M., and Clarke, D. (2004). 'A comparison of the stopping modes for pod-driven ships'. In Proceedings of the 1st International Conference on Technological Advances in Podded Propulsion. Newcastle University, UK, April, pp. 339-356.